













CLASSIFYING THE REACTIVITY OF VOLCANIC ROCKS FROM THE SERRA GERAL GROUP: AN APPROACH USING A PROPOSED REACTIVITY INDEX (RI)

Stephanie Carvalho da Silva¹ , João Pedro Zielinski¹ , Erico Albuquerque Santos¹ , William Jeovanini Fucks¹ , Antônio Rosales Gonçalves Oliveira¹ , Pedro Sousa Costabile¹ , Rodrigo Iglesias¹ , Breno Leitão Waichel² , Victor Hugo Jacks Santos¹ , Felipe Dalla Vecchia¹ , Cassiane Maria Nunes Ferreira³ , Leonildes Soares de Melo Filho³ 

1 - Instituto do Petróleo e dos Recursos Naturais (IPR) - Pontifícia Universidade Católica do Rio Grande do Sul (PUCRS). Av. Ipiranga, 6681, Prédio 96J - Partenon, Porto Alegre - RS, 90619-900. E-mail: stephanie.silva@pucrs.br; joao.zielinski@pucrs.br; erico.santos@pucrs.br; william.fucks@pucrs.br; rosales.antonio@pucrs.br; pedro.costabile@gmail.com; rodrigo.iglesias@pucrs.br; victor.santos@pucrs.br; felipe.vecchia@pucrs.br

2 - Departamento de Geologia - Universidade Federal de Santa Catarina (UFSC). R. Eng. Agrônomo Andrei Cristian Ferreira, s/n - Trindade, Florianópolis - SC, 88040-900. E-mail: breno@cfh.ufsc.br

3 - Repsol Sinopec Brasil. Praia de Botafogo, 300 - Botafogo, Rio de Janeiro - RJ, 22250-040. E-mail: cassiane.ferreira@repsolsinopec.com; leonildes.soares@repsolsinopec.com

Abstract: *The increasing global interest in CO₂ mineralization in basaltic rocks has led to studies within Large Igneous Provinces (LIPs), particularly focusing on their carbon storage potential. In South America, the Serra Geral Group (SGG), part of the Paraná-Etendeka Province, has been the subject of investigations due to its compositional diversity and extensive volcanic sequences. This study assesses the applicability of the Reactivity Index (RI) as a predictive tool for geochemical reactivity in six SGG volcanic rock samples, compared with two Icelandic basalt samples and one of Columbia River Basalt (CRB). Results reveal RI values for SGG samples ranging from -11.1 to -6.7 log mol/s, aligning well with the observations from batch reactor experiments. Higher RI values were associated with increased reactivity, supporting the use of the index as a reliable proxy, especially in preliminary evaluations, although it does not account for textural characteristics or surface area variations. The SGG, Icelandic and CRB samples showed similar RI values. When integrated with petrography, surface area, and chemical data, the RI provides a promising tool for evaluating the reactivity of volcanic rocks in carbon storage strategies.*

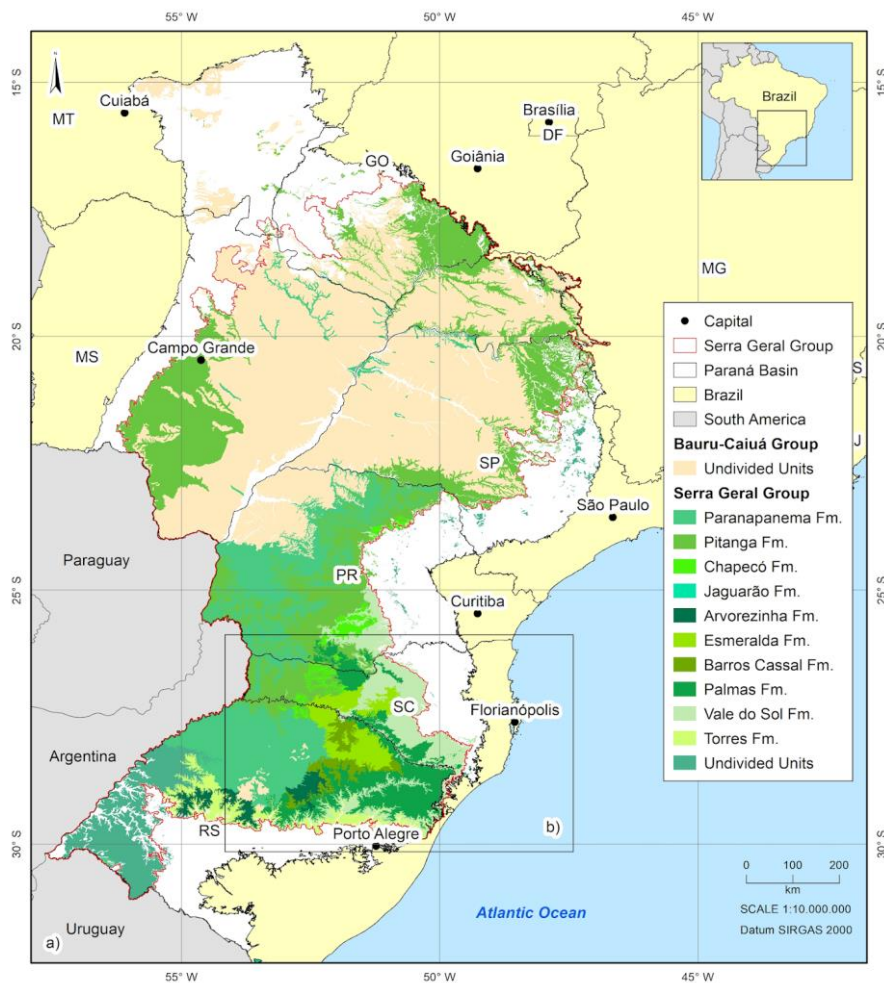
Keywords: *Serra Geral Group; CO₂ mineralization; Reactivity Index; Volcanic rocks reactivity*

1. INTRODUCTION

With the growing global interest in CO₂ mineralization in basaltic rocks, numerous studies have been conducted in Large Igneous Provinces (LIPs) to explore their potential for carbon storage (e.g. Oelkers et al., 2023). In South America, research efforts have focused on the volcanic rocks of the Serra Geral Group (SGG), which is part of the Paraná-Etendeka Large Igneous Province, one of the world's largest LIPs (ca. 135-132 Ma) (Gomes & Vasconcelos, 2021). The SGG covers an area of ~787,000 km² (Fig. 1), and its volcanic rocks comprise a variety of lithologies characterized as basaltic and basaltic andesite rubbly *pāhoehoe* and *pāhoehoe* lava flows, with less predominant dacitic and rhyolitic domes, lava lobes and tabular lava flows (Horn et al., 2022). In addition to chemical and mineral composition variability, the heterogeneity also includes porosity and permeability,

characteristics which may impact CO₂-fluid-rock interactions.

Despite the advances in studies emphasizing the CO₂ mineralization potential (Ferreira et al., 2024; Rossetti et al., 2025), research on the geochemical reactivity of these volcanic rocks remains limited, with substantial knowledge gaps. Although porosity and permeability are important, variations in mineralogical composition also play a key role in reactivity (Rasool & Ahmad, 2023). This study aims to evaluate the applicability of the Reactivity Index (RI), recently proposed by Lu et al. (2024), as a tool for assessing the geochemical reactivity of volcanic rocks from the SGG. To this end, RI values obtained for SGG samples were compared with results from batch reactor experiments using the same materials (Zielinski et al., 2024), as well as with RI values estimated in this study for samples from Icelandic basalts and Columbia River Basalt (CRB).



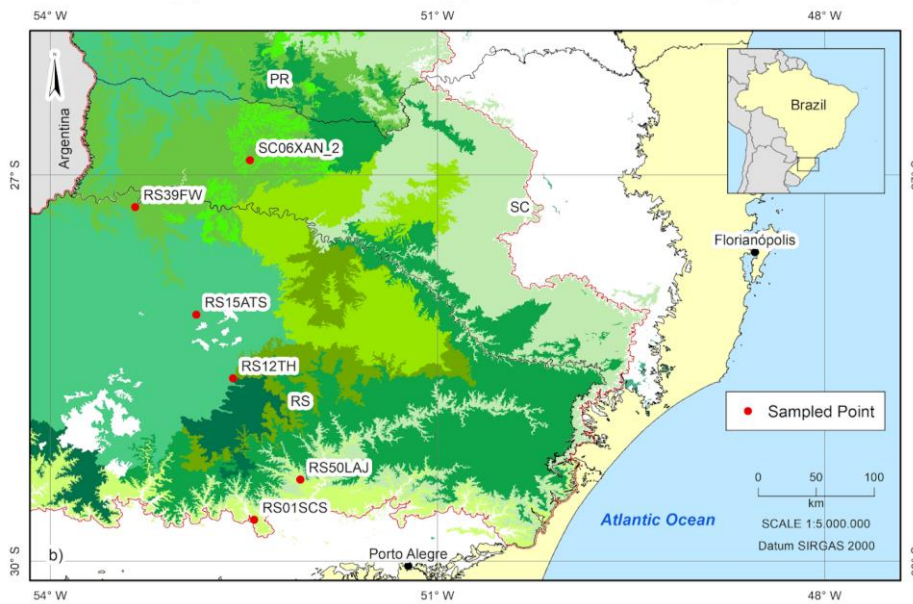


Figure 1 - a) (top) Location of the Serra Geral Group (SGG) within the Paraná Basin. b) (bottom) Sample locations. Based on data from Horn et al. (2022).

2. MATERIALS AND METHODS

To evaluate the RI, a total of six samples from SGG were selected (Fig. 1b). These samples were previously used in batch reactor experiments (Zielinski et al., 2024), and represent distinct compositions and lava flow morphologies, including massive flow core, amygdaloidal/brecciated, and vesicular flow top (Fig. 2). To provide a comparative framework, RI values were also estimated for two Icelandic basalt samples and one from CRB, using compositional data from the literature (Delerce et al., 2023; Adeoye et al., 2017). These rocks are known for their reactivity potential and are important references for comparing with the SGG results.

2.1. Reactivity Index (RI)

The Reactivity Index (RI) was proposed by Lu et al. (2024) and is expressed in Eq (1).

$$RI = \log \log \left(\sum_{i=1}^n \text{Reactivity}_i * f_i \right) \quad (\text{Equation 1})$$

Where i represents each mineral component in the sample. The RI provides a quantitative parameter of the rock's theoretical reactivity based on the logarithmic sum of the reactivity of each mineral component (r_i), weighted by its abundance (f_i). Higher RI values indicate greater reactivity. The r_i were either extracted from published databases (Heřmanská et al., 2022; Heřmanská et al., 2023; Oelkers & Addassi, 2025) or, when not available, were calculated with Eq (2) (Lu et al., 2024) using mineral dissolution rate parameters from Palandri and Kharaka (2004), considering acidic conditions (pH 4.0-4.5) and temperature of 25°C (298 K).

$$\text{Reactivity} = k \exp \left[-\frac{E_a}{R} \left(\frac{1}{T} - \frac{1}{298.15} \right) \right] a_{H^+}^i \quad (\text{Equation 2})$$

Where k is the rate constant, E_a is the activation energy, R is the gas constant, T corresponds to the temperature (K) at which the reaction rate is to be calculated, and a_{H^+} is the activity of the hydrogen ion, directly related to the pH value.

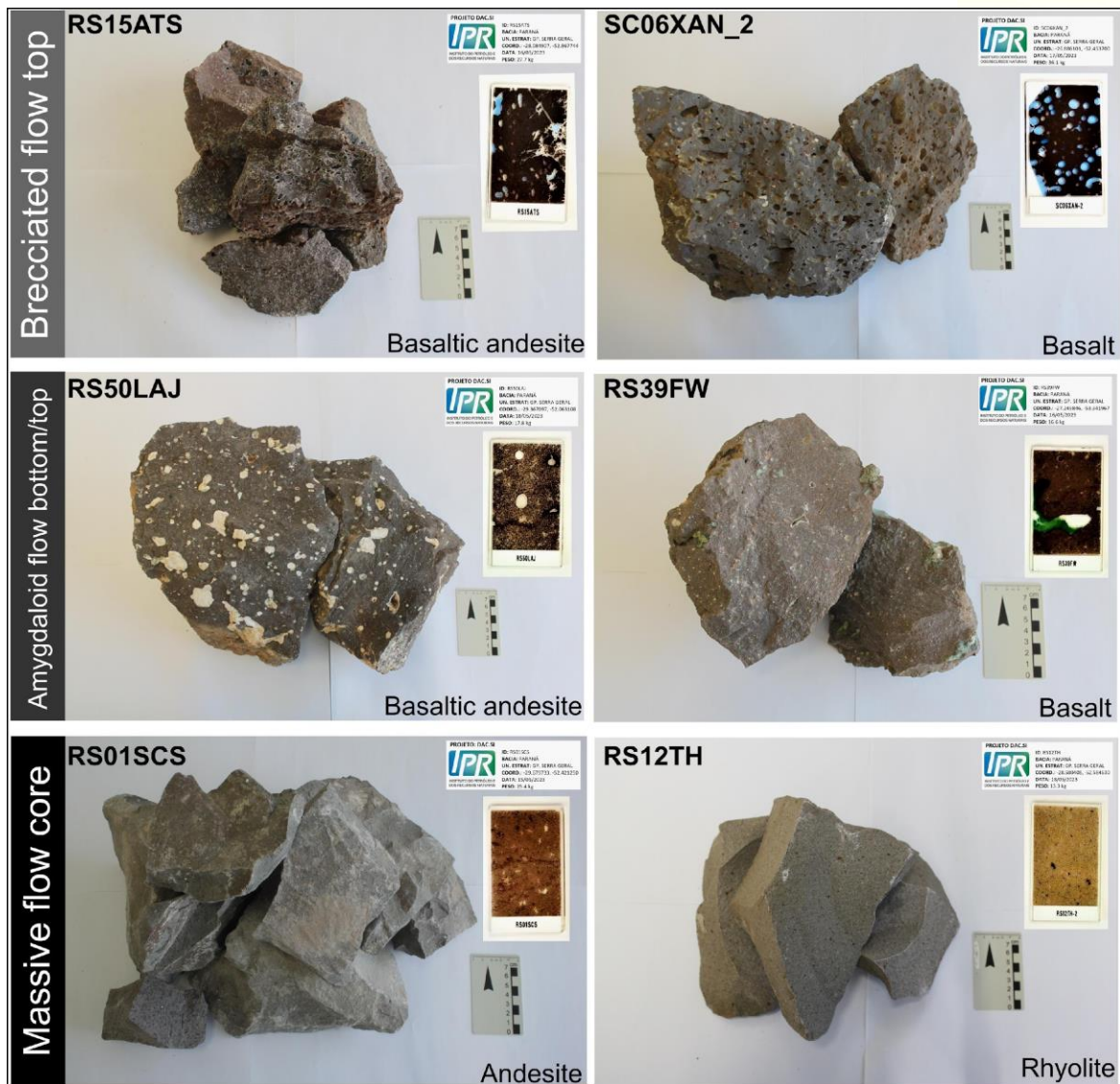


Figure 2 - SGG samples used for RI calculations, representing different lava flow morphologies.

2.2. Sample Characterization

For the SGG samples, petrographic and XRD analysis were conducted to determine the mineralogical composition and phase proportions. All analyses were carried out at the Rock Characterization Laboratory (LCR) of the Institute of Petroleum and Natural Resources (IPR) at PUCRS. Mineralogical data for the two Icelandic basalt samples and the CRB sample were obtained from published works by Delerce et al. (2023) and Adeoye et al. (2017).

Petrographic analyses were performed using optical microscopy, combining qualitative description and quantitative modal analysis by point counting in polished thin sections, using a Leica DM750 microscope. XRD analyses were performed using a BrukerD8 Advance diffractometer (at 40 kV and 30 mA), over an

angular range (2θ) of $3^\circ - 50^\circ$, step size of 0.01, and time of 3 s/step. The data was interpreted using DIFFRAC.EVA 5.0 software for quantitative analyses.

3. RESULTS

3.1. Mineralogical composition

The brecciated flow top samples (SC06XAN_2 and RS15ATS) are fine-grained and plagioclase-phyric, with hypohyaline to aphanitic groundmass. The primary mineral assemblage comprises plagioclase (labradorite), augite, and volcanic glass (>50%), along with variable amounts of opaque minerals. Amygdales (~ 2 to 3 mm) are filled with secondary phases such as zeolite, smectite, celadonite, and calcite. Additionally, RS15ATS contains quartz and olivine (altered to iddingsite).

Amygdaloidal rocks (RS39FW and RS50LAJ) are fine-grained, exhibiting sub-ophitic, intersertal, and hiatal textures, with hypocrySTALLINE aphanitic (RS50LAJ) or hypohyaline (RS39FW) groundmass. The mineral assemblage is predominantly composed of plagioclase (labradorite), augite, volcanic glass, and opaques. Secondary minerals, such as zeolite, celadonite, smectite, chalcedony, and calcite fill amygdales (~ 1 to 7 mm). Olivine, extensively altered and replaced by serpentine minerals (antigorite, chrysotile, lizardite), is also present in sample RS50LAJ.

Among the analysed samples, the massive flow core rocks exhibit distinct textural and mineralogical characteristics compared to the

vesicular varieties. Massive flow core rocks (RS01SCS and RS12TH) are fine-grained and plagioclase-phyric, characterized by sub-ophitic and intersertal textures, with a hypocrySTALLINE aphanitic groundmass. Their mineralogical composition consists of plagioclase (labradorite), augite (intensely altered in sample RS23TH), quartz, volcanic glass and opaque minerals. Sample RS01SCS also contains zeolite and chalcedony-filled amygdales (~ 0.5 mm). Quartz and feldspar intergrowths were observed in RS12TH, as a result of devitrification.

Mineralogical compositions and phase proportions for all samples (including those from the literature) are presented in Table 1.

Table 1 - Sample mineralogy, including phase proportions and mineral reactivity.

Sample	Mineral	n_i (mol/m ² /s)	f_i (0-1)
RS50LAJ	Labradorite	$10^{-10.20}$	0.2029
	Albite	$10^{-11.50}$	0.1062
	Basaltic glass	$10^{-10.60}$	0.2099
	Augite	$10^{-11.60}$	0.2175
	Scolecite	$10^{-8.20}$	0.0320
	Clinoptilolite-Ca	$10^{-10.80}$	0.0710
	Smectite	$10^{-14.12}$	0.0839
	Serpentine	$10^{-11.30}$	0.0764
	TOTAL	-	0.99
RS39FW	Labradorite	$10^{-10.20}$	0.2552
	Albite	$10^{-11.50}$	0.0658
	Basaltic glass	$10^{-10.60}$	0.2804
	Augite	$10^{-11.60}$	0.1655
	Magnetite	$10^{-13.08}$	0.0304
	Hematite	$10^{-14.89}$	0.0541
	Celadonite	$10^{-15.48}$	0.1351
	Calcite	$10^{-4.84}$	0.0135
	TOTAL	-	1.00
SC06XAN_2	Labradorite	$10^{-10.20}$	0.0913

Sample	Mineral	n_i (mol/m ² /s)	f_i (0-1)
	Albite	$10^{-11.50}$	0.0726
	Basaltic glass	$10^{-10.60}$	0.6807
	Augite	$10^{-11.60}$	0.0798
	Magnetite	$10^{-13.08}$	0.0336
	Heulandite-Na	$10^{-10.80}$	0.0420
	TOTAL	-	1.00
RS12TH	Labradorite	$10^{-10.20}$	0.1016
	Albite	$10^{-11.50}$	0.0963
	Orthoclase	$10^{-12.60}$	0.1176
	Sanidine	$10^{-11.60}$	0.0616
	Rhyolitic glass	$10^{-11.50}$	0.1601
	Augite	$10^{-11.60}$	0.0356
	Magnetite	$10^{-13.08}$	0.0320
	Quartz	$10^{-12.70}$	0.3487
	Ilmenite	$10^{-13.85}$	0.0462
	TOTAL	-	0.99
RS01SCS	Labradorite	$10^{-10.20}$	0.1607
	Albite	$10^{-11.50}$	0.0768
	Basaltic glass	$10^{-10.60}$	0.4682
	Augite	$10^{-11.60}$	0.1505
	Ilmenite	$10^{-13.85}$	0.0735
	Ilite	$10^{-14.00}$	0.0689
	TOTAL	-	0.99
RS15ATS	Labradorite	$10^{-10.20}$	0.0991
	Albite	$10^{-11.50}$	0.0474
	Basaltic glass	$10^{-10.60}$	0.5400
	Augite	$10^{-11.60}$	0.0100
	Magnetite	$10^{-13.08}$	0.0148
	Hematite	$10^{-14.89}$	0.0365
	Iddingsite (forsterite)	$10^{-9.08}$	0.0256
	Clinoptilolite-Ca	$10^{-10.80}$	0.1758

Sample	Mineral	n_i (mol/m ² /s)	f_i (0-1)
	Smectite	$10^{-14.12}$	0.0476
	TOTAL	-	1.00
HE-65 W Iceland (Delerce et al., 2023)	Basaltic glass	$10^{-10.60}$	0.1290
	Plagioclase	$10^{-10.20}$	0.3500
	Quartz	$10^{-12.70}$	0.0720
	Augite	$10^{-11.60}$	0.3430
	Amphibole	$10^{-10.70}$	0.0170
	Chlorite	$10^{-11.80}$	0.0730
	Magnetite	$10^{-13.08}$	0.0170
	TOTAL	-	1.00
GOB_14 E Iceland (Delerce et al., 2023)	Basaltic glass	$10^{-10.60}$	0.2020
	Labradorite	$10^{-10.20}$	0.3300
	Diopside	$10^{-10.30}$	0.2850
	Pigeonite	$10^{-11.60}$	0.0750
	Chlorite	$10^{-11.80}$	0.0050
	Chabazite	$10^{-10.80}$	0.0040
	Analcime	$10^{-8.24}$	0.0430
	Thomsonite	$10^{-8.20}$	0.0350
	Levyne	$10^{-10.80}$	0.0080
	Ilmenite	$10^{-13.85}$	0.0130
	TOTAL	-	1.00
UB Columbia River (Adeoye et al., 2017)	Diopside	$10^{-10.30}$	0.2000
	Forsterite	$10^{-9.08}$	0.1300
	Fayalite	$10^{-9.70}$	0.1900
	Antigorite	$10^{-11.10}$	0.0200
	Albite	$10^{-11.50}$	0.0400
	Anorthite	$10^{-10.20}$	0.0500
	K-feldspar	$10^{-10.70}$	0.3500
	TOTAL	-	0.98

3.2. Estimated Reactivity Index (RI)

The calculated RI values for SGG samples ranged from -11.12 to -6.71 log mol/s, with an average of -9.80 log mol/s. Sample RS39FW revealed the highest RI with -6.71 log mol/s and sample RS12TH showed the lowest RI, with a value of -11.12 log mol/s. Samples RS50LAJ, RS15ATS, SC06XAN_2, RS01SCS revealed RI values of -9.65, -10.36, -10.62 and -10.64 log mol/s, respectively. For the Iceland basalt samples, the RI values were -9.29 and -10.57 log mol/s, whereas the CRB sample revealed -9.77 log mol/s.

Based on the RI values, the samples were grouped according to their relative reactivity (Fig. 3): i) those with $RI > -8.00$ were considered highly reactive; ii) those with $-9.90 < RI \leq -9.00$ were considered to have intermediate

reactivity; iii) those with $-10.90 < RI \leq -10.00$ were regarded as having low-to-intermediate reactivity; and iv) those with $RI \leq -10.90$ were considered to have very low reactivity. The RI value of sample RS39FW (-6.71 log mol/s) was approximately four orders of magnitude higher than that of the least reactive sample. Samples GOB_14 (-9.29 log mol/s) from Iceland, RS50LAJ (-9.65 log mol/s) and UB from CRB (-9.78 log mol/s) revealed intermediate reactivity. Samples RS15ATS, SC06XAN_2, and RS01SCS showed moderate/intermediate reactivity. Among all samples, RS12TH (-11.12 log mol/s) stood out as the least reactive, with an RI nearly one order of magnitude lower than the intermediate reactivity samples and slightly lower than the other low reactivity samples.

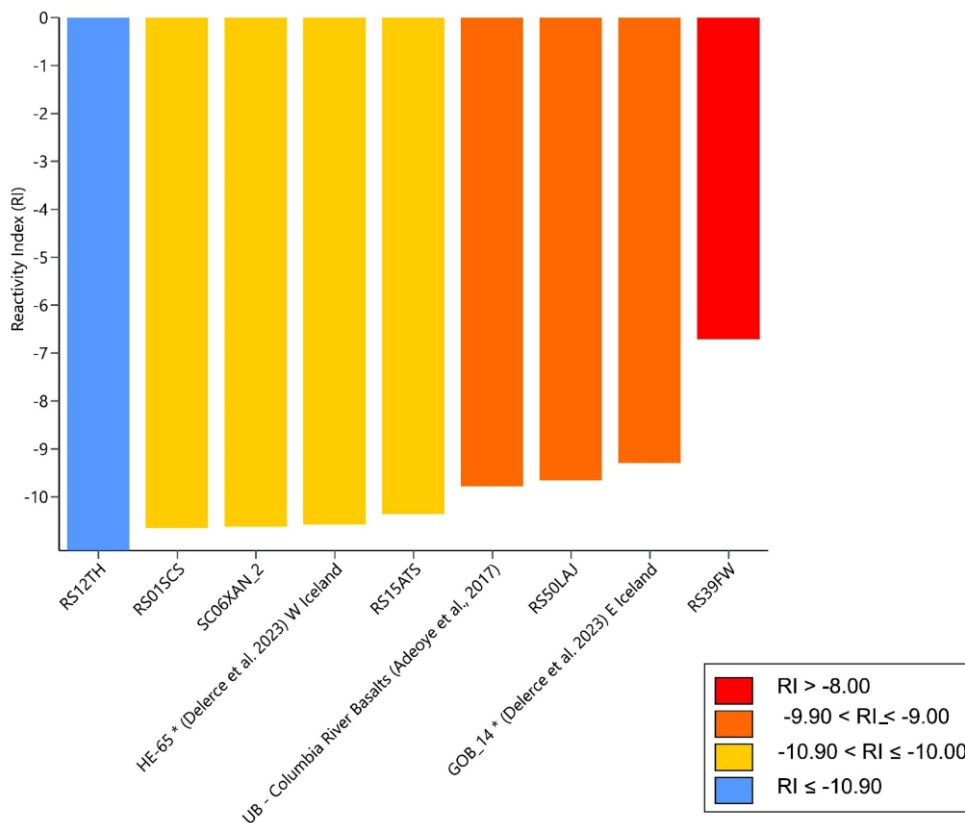


Figure 3 - Sample reactivity groups based on the RI values.

4. DISCUSSIONS

The range of RI values for SGG samples indicates substantial variation in their reactivity. The RI of sample RS39FW suggests it is the most reactive among the analysed basalts. This result aligns with the experimental findings reported in Zielinski et al. (2024), where RS39FW exhibited strong pH buffering capacity (initial average pH of 8.8 units, stabilizing at ~4.5), elevated electrical conductivity (EC > 1500 $\mu\text{S}/\text{cm}$) - consistent with ion release into solution, and total alkalinity (TA) values > 950 mg/L. According to the authors, this sample also reached more than 150 mg/L of Ca concentrations in solution during the experimental period (45 days), at least twice the amount observed in the other samples (15 to 75 mg/L).

In contrast, sample SC06XAN_2 presented a low RI value (-10.62 log mol/s), positioning it among the least reactive samples, based on the RI. However, according to experimental observations, this sample was grouped with RS39FW, considering the similar pH stabilization, elevated EC and TA values, and Ca and Mg concentrations. This inconsistency between the RI and the observed reactivity may reflect limitations of the index. Potential causing factors include mineral crystallinity and surface properties (reactive surface area - RSA), or specific kinetic effects that are not fully captured by the RI approach. Although the volcanic glass phase was included in the RI calculation using specific r_i from databases, the RI may not reflect differences between the glass present in the sample and in the database reference. Variations in glass composition and hydration, for example, can influence the dissolution behavior (Wolff-Boenisch et al., 2004). Furthermore, the RI does not account for differences in the reactive surface area (RSA). Textural factors such as grain size, particle roughness, porosity, and surface fracturing can increase RSA, accelerating reaction rates in ways not captured by the bulk mineralogical composition. These combined effects may help explain the experimental

reactivity observed for SC06XAN_2, despite its low RI.

On the other hand, sample RS50LAJ (-9.65 log mol/s), which showed an intermediate RI, exhibited moderate increases in EC (by a factor of ~2.2) and TA (by a factor of ~3.3), with a slightly higher Ca release, when compared to samples RS15ATS, RS01SCS, and RS12TH, according to the experimental results reported by Zielinski et al. (2024). Samples RS15ATS (-10.36 log mol/s), RS01SCS (-10.64 log mol/s), and RS12TH (-11.12 log mol/s) were grouped as having lower reactivity, as evidenced by limited pH buffering (reaching values around 4.0) and smaller increases of EC, TA, and Ca concentrations during the first 3-7 days. The authors also reported some variability within this group, particularly related to Mg release, with Mg concentrations progressively increasing in samples RS15ATS and RS12TH over time. These observations are consistent with their classification as lower reactivity samples, according to the RI-based grouping.

Despite initial theoretical and experimental discrepancies, the results from this RI-based approach suggest that SGG volcanic rocks have a reactivity potential similar to Icelandic and CRB basalts, supporting their feasibility for CO₂ mineralization.

5. CONCLUSIONS

The RI values of the SGG samples were consistent with some experimental observations, indicating a favorable correlation and supporting the use of the RI for assessing reactivity. The overall consistency between RI values and experimental data reinforces the potential applicability of the RI as a reliable metric for reactivity assessment. Although RI values are based on mineralogical composition and established kinetic factors, without accounting factors like surface texture or reactive surface area (RSA), its use should be seen as a screening tool. When the RI is applied in an integrated approach - including other methods such as petrographic analysis, chemical data, reactive surface area studies - its effectiveness can be enhanced and it can

provide useful insights for evaluating the potential reactivity of rocks.

6. REFERENCES

- ADEOYE, J. T.; MENEFE, A. H.; XIONG, W.; WELLS, R. K.; SKEMER, P.; GIAMMAR, D. E.; ELLIS, B. R. Effect of transport limitations and fluid properties on reaction products in fractures of unaltered and serpentinized basalt exposed to high PCO₂ fluids. *International Journal of Greenhouse Gas Control*, v. 63, p. 310–320. Disponível em: <https://doi.org/10.1016/j.ijggc.2017.06.003> .
- DELERCE, S.; BÉNÉZETH, P.; SCHOTT, J.; OELKERS, E. H. The dissolution rates of naturally altered basalts at pH 3 and 120°C: Implications for the in-situ mineralization of CO₂ injected into the subsurface. *Chemical Geology*, v. 621, art. 121353. Disponível em: <https://doi.org/10.1016/j.chemgeo.2023.121353> .
- FERREIRA, A.; SANTOS, R. V.; DE ALMEIDA, T. S.; CAMARGO, M. A.; ANDRÉ FILHO, J.; MIRANDA, C. R.; DOS PASSOS, S. de T. A.; BAPTISTA, A. D. T.; TASSINARI, C. C. G.; RUBIO, V. A.; CAPISTRANO, G. G. Unraveling the rapid CO₂ mineralization experiment using the Paraná flood basalts of South America. *Scientific Reports*, v. 14, art. 8116. Disponível em: <https://doi.org/10.1038/s41598-024-58729-w> .
- GOMES, A. S.; VASCONCELOS, P. M. Geochronology of the Paraná-Etendeka large igneous province. *Earth-Science Reviews*, v. 220, art. 103716. Disponível em: <https://doi.org/10.1016/j.earscirev.2021.103716> .
- HEŘMANSKÁ, M.; VOIGT, M. J.; MARIENI, C.; DECLERCQ, J.; OELKERS, E. H. A comprehensive and consistent mineral dissolution rate database: Part I: Primary silicate minerals and glasses. *Chemical Geology*, v. 597, art. 120807. Disponível em: <https://doi.org/10.1016/j.chemgeo.2022.120807> .
- HEŘMANSKÁ, M.; VOIGT, M. J.; MARIENI, C.; DECLERCQ, J.; OELKERS, E. H. A comprehensive and consistent mineral dissolution rate database: Part II: Secondary silicate minerals. *Chemical Geology*, v. 636, art. 121632. Disponível em: <https://doi.org/10.1016/j.chemgeo.2023.121632> .
- HORN, B. L. D.; OLIVEIRA, A. A.; SIMÕES, M. S.; BESSER, M. L.; ARAÚJO, L. L. Mapa geológico da Bacia do Paraná. CPRM/SGB. Disponível em: <https://rigeo.sgb.gov.br/handle/doc/23037> .
- LU, P.; APPS, J.; ZHANG, G.; GYSI, A.; ZHU, C. Knowledge gaps and research needs for modeling CO₂ mineralization in the basalt-CO₂-water system: A review of laboratory experiments. *Earth-Science Reviews*, v. 254, art. 104813. Disponível em: <https://doi.org/10.1016/j.earscirev.2024.104813> .
- OELKERS, E. H.; ADDASSI, M. A comprehensive and consistent mineral dissolution rate database: Part III: Non-silicate minerals including carbonate, sulfate, phosphate, halide, and oxy-hydroxide minerals. *Chemical Geology*, v. 673, art. 122528. Disponível em: <https://doi.org/10.1016/j.chemgeo.2024.122528> .
- OELKERS, E. H.; GISLASON, S. R.; KELEMEN, P. B. Moving subsurface carbon mineral storage forward. *Carbon Capture Science & Technology*, v. 6, art. 100098. Disponível em: <https://doi.org/10.1016/j.ccst.2023.100098> .
- PALANDRI, J. L.; KHARAKA, Y. K. A compilation of rate parameters of water-mineral interactions kinetics for application to geochemical modeling. U. S. Geological Survey. Disponível em: <https://doi.org/10.3133/ofr20041068> .
- RASOOL, M. H.; AHMAD, M. Reactivity of basaltic minerals for CO₂ sequestration via in situ mineralization: A review. *Minerals*, v. 13, n. 9, art. 1154. Disponível em: <https://doi.org/10.3390/min13091154> .
- ROSSETTI, L. M. M.; MILLETT, J. M.; ROSSETTI, M. M. M.; MARINS, G. B.; SIMÕES, M. S.; MANTON, B.; CARMO, I. de O.; DE LIMA, E. F. Subsurface geology of the Paraná-Etendeka Large Igneous Province: Implications to province stratigraphy and CO₂ storage. *Basin Research*, v. 37, n. 3, art. e70038. Disponível em: <https://doi.org/10.1111/bre.70038> .
- WOLFF-BOENISCH, D.; GISLASON, S. R.; OELKERS, E. H.; PUTNIS, C. V. The dissolution rates of natural glasses as a function of their composition at pH 4 and 10.6, and temperatures from 25 to 74°C. *Geochimica et Cosmochimica Acta*, v. 68, n. 23, p. 4843–4858. Disponível em: <https://doi.org/10.1016/j.gca.2004.05.027> .
- ZIELINSKI, J. P.; DOS SANTOS, E. A.; DA SILVA, S. C.; FUCKS, W. J.; OLIVEIRA, A. R. G.; MULLER, L. de S.; IGLESIAS, R.; WAICHEL, B. L.; SANTOS, V.; MELO, C.; VECCHIA, F. D.; NUNES, C.; FILHO, L. S. de M. Initial insights into the geochemical reactivity of volcanic rocks from the Serra Geral Group (Paraná Basin, Brazil): A laboratory-scale perspective on in-situ mineralization. *SSRN Electronic Journal*. Disponível em: <https://dx.doi.org/10.2139/ssrn.5059245> .

Editado por Luana Tiemi Moletta (PET-GEOLOGIA/UFPR)